

11,12

Numerical simulation of the behavior of enstatite up to 1.4 TPa

© K.K. Maevskii

Lavrentyev Institute of Hydrodynamics, Siberian Branch, Russian Academy of Sciences,
Novosibirsk, Russia

E-mail: konstantinm@hydro.nsc.ru

Received March 17, 2023

Revised April 21, 2023

Accepted April 23, 2023

An accurate description of the effect of extreme pressure and temperature on the physical properties of materials is required to understand the structure and composition of the mantle of the Earth and similar planets. One of such materials is enstatite MgSiO_3 , which causes increased interest in the investigating of its behavior under intense dynamic loads. It is proposed to consider the shock-wave loading of enstatite as a mixture of quartz oxides SiO_2 and MgO periclase in an equal stoichiometric ratio based on experimental data in which decomposition of magnesium silicates was observed. Calculations are performed using a thermodynamically equilibrium model that takes into account the phase transitions of the components. Phase transitions of SiO_2 and MgO are taken into account when modeling high-energy effects on enstatite. The results are compared with the data obtained on the basis of shock-wave loading experiments, as well as with calculations based on the PREM model performed based on the results of seismic exploration.

Keywords: equation of state, phase transitions, quartz oxide, periclase oxide, enstatite.

DOI: 10.21883/PSS.2023.06.56119.38

1. Introduction

Fundamental issues of structure, dynamics and evolution of the mantle of the Earth and new exoplanets are solved with the help of numerous experiments on geological materials at high pressures and temperatures corresponding to those expected in the planets' interior [1,2]. In particular, the investigations of phase equilibria determined various phases of silicates and oxides at high pressure [3,4]. *Ab initio* calculations performed for enstatite MgSiO_3 show that this mineral shall dissociate into MgO and SiO_2 at pressures and temperatures that are expected on the terrestrial exoplanets [5]. Previous experiments [6] in the region of 33 GPa have already shown such dissociation for Mg_2SiO_4 into MgO and SiO_2 in the form of stishovite, because SiO_2 is transformed into stishovite at pressures higher than 10 GPa [7]. Simulated compositions of mantle materials with six components were investigated in [8]: CaO , FeO , Na_2O , Al_2O_3 , MgO , SiO_2 . In this context, it was noted that MgO and SiO_2 contribute the major share to the mantle materials composition. To understand the impacts of extreme pressures and temperatures, exact description of their influence on physical properties of the component materials is required, which necessitates further experimental and theoretical investigations. Phase relations and other calculated data were investigated in [9] at pressures up to 12 GPa and temperatures up to 2000 K for MgSiO_3 . Impact tests on MgSiO_3 with pressures up to 1400 GPa and sample densities more than 9 g/cm^3 are described in [10]. Experiments for the study of phase diagrams at high pressures and phase transitions in $\text{MgO}-\text{SiO}_2$ are described in [11]. Experimental data

on compression of MgSiO_3 crystals up to 400 GPa and equations of state for pressures up to 950 GPa are provided in [12]. Equations of state for MgSiO_3 and phase diagram of Mg_2SiO_4 at pressures up to 130 GPa were provided in [13].

Great attention is paid to the possibility of phase transition of the studied magnesium silicates [13]. Thus, [14] attributes such high interest in this materials to the fact that such materials as MgO , MgSiO_3 and Mg_2SiO_4 are one of the most essential finite elements of the Earth's mantle and similar planets. Therefore, detailed knowledge of the phase diagram of these magnesium finite elements is essential for correct simulation of the planets' interior structures. As a result, phase diagrams shall be studied in wider pressure and temperature ranges using, in particular, dynamic compression methods. Various theoretical and experimental investigations of dynamically compressed magnesium silicate phases have been carried out recently, but some contradictions have not been resolved yet [14]. In [15], molecular dynamics simulation was used for *ab initio* calculations of physical properties of MgO in conditions extending from those occurring in the Earth's mantle to those expected for giant planets such as Jupiter.

2. Problem formulation

The idea that the Earth's mantle is composed of decomposition products of ferro-magnesian silicates into MgO , SiO_2 and small amounts of FeO is verified in [16] using the information obtained from the shock wave compression experiments carried out on periclase and SiO_2 up to

250 GPa. It is assumed that abnormal density growth may be attributed to phase transitions of silicates. According to these assumptions and experimental data on magnesium silicate dissociation into MgO and SiO₂ [6], that were obtained at pressures near phase transition of SiO₂, an assumption was made that phase transitions of magnesium silicates are determined by phase transitions of components into which the initial materials decompose at appropriate pressures. To verify this description of such processes, a model shall be provided to calculate the behavior of mixtures with components undergoing phase transition under high dynamic loads. Additive approximation is the most commonly used method which assumes the volume of shock-compressed mixture equal to the sum of volumes of components achieved by separate shock compression at the same pressure. Satisfactory data was obtained for solid samples [17]. However, the rule of additivity in this approach is approximate, because it assumes unreal identity between compression of heterogeneous mixture components and shock compression of components. Problems also occur in the presence of phase transitions in samples. In particular, an attempt to restore shock adiabat of SiO₂ [18] by the shock adiabat of the mixture of aluminium and SiO₂ and the shock adiabat of pure aluminium using the additive model was not successful. This was because the experimental data obtained for the high pressure phase in which the substance exists after the phase transition corresponds to the shock adiabat of the high pressure phase with the initial sample density. Taking into account that the high pressure phase density is higher than the low pressure phase density, calculation of the shock adiabat of a porous substance is actually necessary and, therefore, an equation of state is required, as appropriate.

For materials undergoing phase transition, a thermodynamically equilibrium model is used [19]. Shock wave impact calculations for Mg₂SiO₄ that is considered to be a mixture of SiO₂ and MgO are provided in [20,21]. The model is based on the assumption that mixture components exposed to shock wave loading are in thermodynamic equilibrium, i.e. component temperature equality is also considered. For a two-phase medium, this assumption was used in [22]. The proposed model reliably describes the high-intensity impact on materials in a wide pressure range, including for SiO₂ and MgO [23,24]. Consideration of the mixture component temperature equality enables the mixture shock adiabats to be calculated within the experiment accuracy limits [25,26]. In the phase transition region, the sample is treated as a mixture of low pressure and high pressure phases in order to reliably describe the region of polymorphous phase transition for the substances in question [27]. Now it is possible to describe thermodynamic properties of mixtures containing components that undergo phase transition when exposed to a shock wave impact.

3. Calculation model

The Mie–Grüneisen type equation of state is used to describe the behavior of the condensed phases as follows:

$$P(\rho, T) = P_C(\rho) + P_T(T), \quad (1)$$

$$P_T(\rho, T) = \Gamma \rho E_T(T), \quad E_T(T) = c_V(T - T_0). \quad (2)$$

Here, P_C is the potential pressure component, P_T , E_T are the thermal components of pressure and specific energy, c_V is the thermal capacity, T_0 is the initial temperature. Cold pressure component P_C is described by the following equation: $P_C(\rho/\rho_0) = A((\rho/\rho_0)^k - 1)$, (ρ , ρ_0 is the current and initial density of the condensed component, A , k are the coefficients of the equation of state). For gas in case of porous materials, ideal gas equation of state is used. mass-flow conservation conditions for each mixture component and momentum and energy conservation conditions for the mixture as a whole are established. For material composed of n solid components with initial volume ratios μ_{i0} , the following dependence of pressure on component compression may be derived:

$$P = \left(\sum_{i=1}^n A_i \frac{\mu_{i0}}{\sigma_i} \left[\left(h_i - \frac{k_i + 1}{k_i - 1} \right) \sigma_i^{k_i} + \frac{2k_i \sigma_i}{k_i - 1} - h_i - 1 \right] \right) / P1,$$

$$P1 = \sum_{i=1}^n \frac{\mu_{i0}}{\sigma_i} h_i + \left(\frac{h_g}{\sigma_g} \right) \left(1 - \sum_{i=1}^n \mu_{i0} \right) - 1. \quad (3)$$

With $h_i = 2/\Gamma_i + 1$; $h_g = 2/(\gamma - 1) + 1$. $\sigma_i = \rho_i/\rho_{i0}$ are compression ratios of condensed component $i = 1, \dots, n$, $\sigma_g = \rho_g/\rho_{g0}$, and ρ_g , ρ_{g0} are current and initial gas densities, adiabatic exponent $\gamma = 1.41$. Temperature-dependent function $\Gamma = P_TV/E_T$, which defines the contribution of thermal components, is introduced into the equation of state to describe the high-intensity impact on materials with different porosity [19]. Consideration of dependence of function Γ on temperature allowed to describe reliably the shock wave loading results for solid and porous samples, which is essential for calculations taking into account phase transitions in wide pressure and porosity ranges. Using the component temperature equality and equations of state of each component, shock adiabats of the multicomponent mixture are calculated.

In the phase transition region, volume ratio α of the low pressure phase changes to the high pressure phase, and it was shown before that dependence α on the internal energy is near-linear. According to the experimental findings, the pressure corresponding to the phase transition process onset is determined. The shock adiabat calculations address three simulation sections for materials undergoing polymorphous phase transition. Before the start of phase transition $\alpha = 0$; in the second section, α grows linearly in function of internal energy $\alpha = (E - E_b)/kf$, whereby $kf = E_f - E_b$, (E is the current internal energy, E_b is the internal energy at the phase transition onset, E_f is the internal energy, when the whole material has entered the high pressure

Phase transition onset parameters

Material	P_f , GPa	k_f , kJ/g
SiO ₂	11	2.50
MgO	325	2.50

phase). The end of phase transition is determined by full transition of the low pressure phase into the high pressure phase, further calculation is carried out at $\alpha = 1$. It should be noted that k_f that correlates volume ratio α with the internal energy and found for one porosity value also allows reliable description of other porosity values of the material in question. Pressures at which phase transition P_f starts and k_f are listed in the Table.

4. Simulation results

Calculation of shock adiabats for low pressure phase of MgOI and high pressure phase of MgOII, as well as the curve describing MgO phase transition region in pressure–density variables are shown in Figure 1. Data obtained from experiments [28,29] and dependence of pressure on the Earth’s mantel density obtained from PREM model are also shown here [30]. Boundaries of SiO₂ and MgO phase transition regions and pressure in the Earth’s center are given for comparison.

To verify the description reliability of oxide mixtures with other materials, calculations were carried out for the

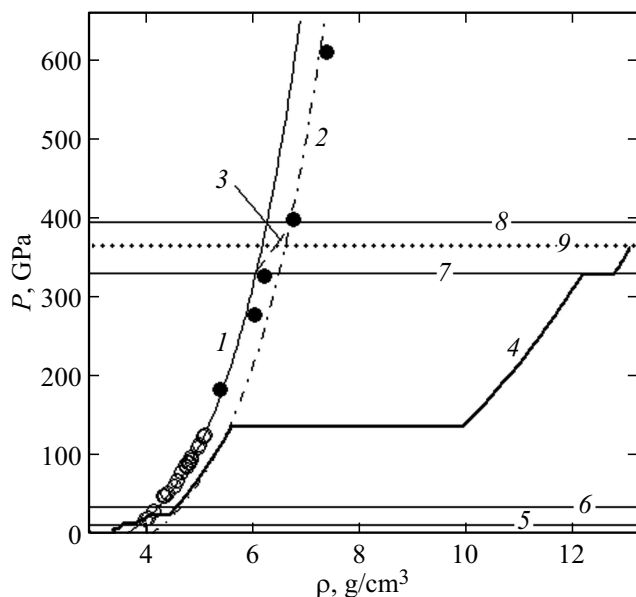


Figure 1. shock adiabats for MgO. Calculated curves: 1 — MgOI, 2 — MgOII, 3 — phase transition of MgO, 4 — PREM data [30]; solid lines: 5 — phase transition onset of SiO₂, 6 — end; 7 — phase transition onset of MgO, 8 — end; 9 — pressure in the Earth’s center. Data: light circles [28], dark circles [29].

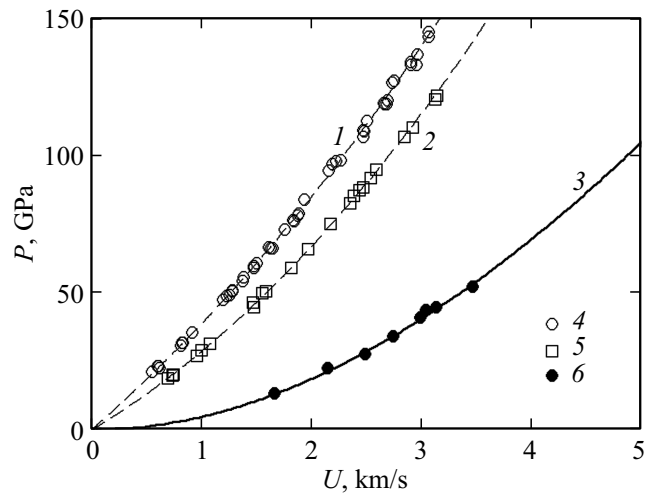


Figure 2. shock adiabats of periclase, corundum and mixture of MgO and Al₂O₃. Calculation: curve 1 — MgO, 2 — Al₂O₃, 3 — mixture of MgO and Al₂O₃. Data: 4, 5, 6 [31].

mixtures for which shock-wave loading test findings were available. Using the parameters found for oxides [20], data for such samples at the experiment accuracy level were described consistently.

Simulation results of shock adiabats of periclase MgO, corundum Al₂O₃ and their mixture in equal molar volumes with density $\rho_0 = 2.118 \text{ g/cm}^3$ compared with data [31] in pressure — mass rate coordinates are shown in Figure 2. Taking into account the experimental pressure range up to 150 GPa, these calculations were carried out for the low pressure phase of MgO. Calculations for the mixture components in question are also given there. The simulation results correspond to the experimental data for pure oxides and their mixture.

Similar calculations were carried out for various mixture compositions, including SiO₂ as a component. Simulation of shock adiabats of SiO₂ mixtures with metals compared with data [32,33] in the pressure–compression coordinates are shown in Figure 3. The calculations were carried out for quartz and tungsten mixture with density $\rho_0 = 10.19 \text{ g/cm}^3$ and quartz and aluminium mixture with $\rho_0 = 2.684 \text{ g/cm}^3$. For these mixtures, the calculation was carried out up to 200 GPa. The calculation curve for the aluminium mixture is given with compression shift by 0.2, for clarity. In this range, SiO₂ undergoes phase transition, stishovite is assumed as the high pressure phase. Similar to [20], it is assumed that quartz, bypassing the intermediate coesite phase, changes directly to stishovite. The thermodynamic parameter calculation for the mixture taking into account phase transition of SiO₂ after the end of phase transition above 40 GPa has been, therefore, carried out for the tungsten, aluminium and stishovite mixtures. Taking into account the observed dissociation of Mg₂SiO₄ into MgO and SiO₂ in the form of stishovite at 33 GPa [6], it can be assumed that stishovite will be also present for enstatite at this pressure. Calculations do not contradict with

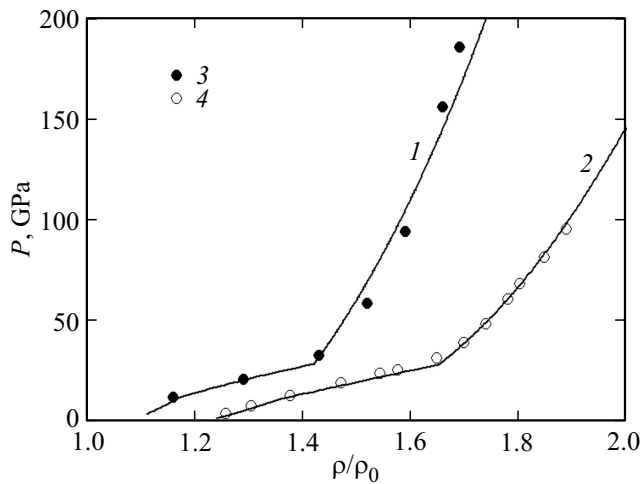


Figure 3. shock adiabats of SiO₂ mixtures. Calculation: curve 1 — mixture of SiO₂ and tungsten, 2 — mixture of SiO₂ and aluminium. Data: 3 [32], 4 [33].

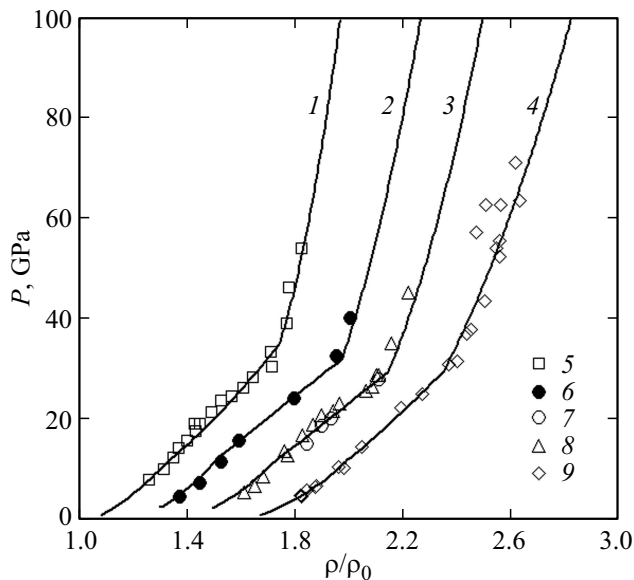


Figure 4. shock adiabats of SiO₂ mixtures. Calculation: curve 1 — mixture with PTFE; 2, 3 — with paraffin, 4 — with epoxy resin. Data: 5, 8 [34], 6, 9 [31], 7 [35].

this assumption. According to the calculation, at 33 GPa, most of SiO₂ has changed to the high pressure phase.

Calculations for various mixtures of organic materials and SiO₂ as a component, and experimental data [31,34,35] are shown in Figure 4. Using the proposed approach, experimental shock-wave loading results for mixtures of SiO₂ with PTFE — $\rho_0 = 2.38 \text{ g/cm}^3$ (curve 1); with paraffin — $\rho_0 = 1.92 \text{ g/cm}^3$ (curve 2), $\rho_0 = 1.78 \text{ g/cm}^3$ (curve 3); with epoxy resin — $\rho_0 = 1.66 \text{ g/cm}^3$ (curve 4) are described consistently. Calculation curve 2 for the mixture with paraffin is given with compression shift by 0.2, curve 3 is given with shift 0.4, curve 4 is given with shift 0.6. The possibility of simulating the parameters of a mixture with

two components undergoing phase transition under shock-wave loading is shown in [24]. Reliable description of the available experimental data was obtained.

Using the experimental data reporting dissociation of magnesium silicates under pressure, assumption on possibility of considering these materials as oxide mixtures was verified. Shock-wave loading of mixture of SiO₂ and MgO with corresponding stoichiometric ratio 1:1 was simulated and compared with the experimental data for enstatite. The simulation results for with $\rho_0 = 3.01 \text{ g/cm}^3$ samples are shown in Figure 5 in the wave rate — mass rate coordinates. Porosity defined as the ratio of solid material density and sample density, $m = 1.03$, was calculated by the mean value of samples used in the experiments. The data of two groups of experiments for samples with a mean density of 3.01 and 2.95 g/cm³ [31] are also shown here. The deviation, in particular, is explained by the density scatter.

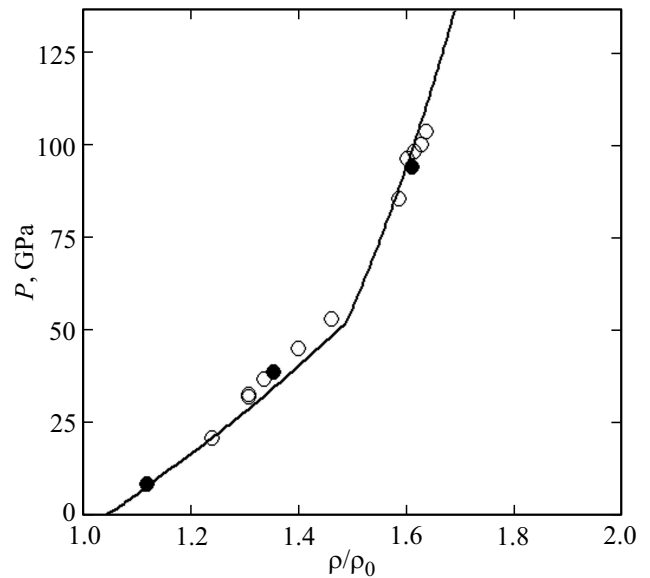


Figure 5. Shock adiabat of enstatite. Calculation — solid curve. Data: [31].

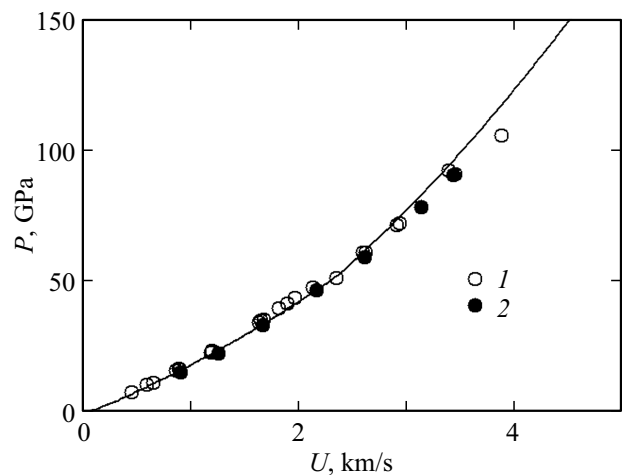


Figure 6. shock adiabat of porous enstatite. Calculation — solid curve. Data: [31].

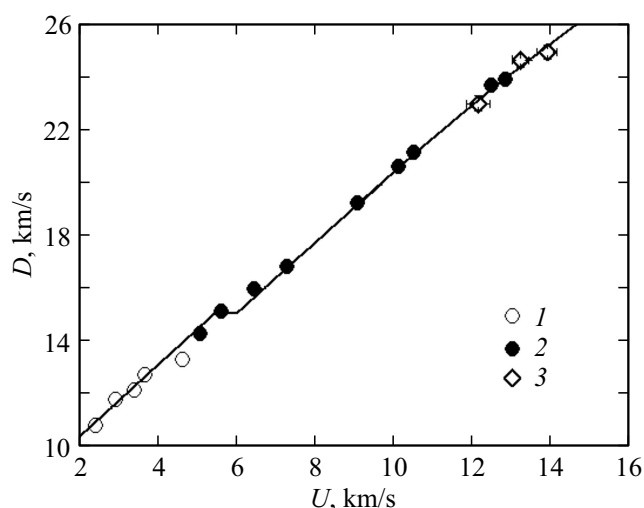


Figure 7. Shock adiabat of enstatite. Calculation — solid line. Data: 1 [35], 2 [36], 3 [37].

Simulation results for porous enstatite samples with $\rho_0 = 2.836 \text{ g/cm}^3$, with this $m = 1.1$, are shown in Figure 6. Data obtained experimentally are also shown [31]. Taking into account the data range, Figure 5, 6, used to verify the calculations up to 120 GPa, simulation was carried out in view of phase transition of SiO_2 .

The calculation for the enstatite samples with $\rho_0 = 4.10 \text{ g/cm}^3$ covering the range up to 1400 GPa and the experimental data [10,37,38] is shown in Figure 7. In this case, phase transition of MgO is considered. The calculations carried out using the thermodynamically equilibrium model have proved the possibility of simulating high-energy loading of magnesium silicates considered as a mixture of SiO_2 and MgO with the appropriate stoichiometric ratio. For MgSiO_3 this is 1:1, for Mg_2SiO_4 this is 1:2 as shown earlier in [20].

5. Conclusion

Taking into account the experimentally observed dissociation of magnesium silicates into MgO and SiO_2 [6], it can be assumed that the phase transition of SiO_2 into stishovite contributes to the density modification of the Earth's upper mantle near 30 GPa that corresponds to the phase transition of SiO_2 . The Earth's mantle density jump near 330 GPa according to [30] corresponds to the phase transition region of MgO. Based on the analysis of the available data, P_f for MgO was corrected up to 325 GPa compared with [20]. Phase transition region of MgSiO_3 from the low pressure phase to the high pressure phase was defined within 300–400 GPa [38] and justifies the suitability of this value P_f . It has been shown that by considering magnesium as a mixture of components under high dynamic loads, behavior of the studied material within the pressure range up to 1.4 TPa can be described reliably. Description of a complex substance as a mixture of components for

carbides is provided in [20]. The proposed model provides reliable description of phase transitions of all components of the material in question. Additional experimental data could help define the phase transition region of components and clarify the question of high pressure phase transition for SiO_2 that has been discussed or a long time.

Compatibility of the model calculations to the results obtained experimentally for MgSiO_3 shows that the used technique may be helpful to describe reliably the behavior of materials undergoing phase transitions under high-intensity loads.

Funding

The study was supported by state assignment for R & D, No. 2021-0006.

Conflict of interest

The author declares that he has no conflict of interest.

References

- [1] W.J. Borucki. Rep. Prog. Phys. **79**, 3, 036901 (2016).
- [2] P.E. Driscoll. Planetary Interiors, Magnetic Fields, and Habitability. In: Handbook of Exoplanets / Eds H. Deeg, J. Belmonte. Springer, Cham (2018).
- [3] T. Gasparik. Phase Diagrams for Geoscientists. Springer, N. Y. (2014). 462 p.
- [4] A.R. Oganov, R. Martoňák, A. Laio, P. Raiteri, M. Parrinello. Nature **438**, 04439, 1142 (2005).
- [5] K. Umemoto, R.M. Wentzcovitch, P.B. Allen. Sci. **311**, 5763, 983 (2006).
- [6] M. Kumazawa, H. Sawamoto, E. Ohtani, K. Mazaki. Nature **247**, 356 (1974).
- [7] E. Ohtani. Annu. Rev. Earth. Planet. Sci. **49**, 253 (2021).
- [8] W. Xu, C.L. Bertelloni, L. Stixrude, J. Ritsema. Earth. Planet. Sci. Lett. **275**, 78 (2008).
- [9] T.S. Sokolova, P.I. Dorogokupets, A.I. Filippova. Phys. Chem. Minerals **49**, 9, 37 (2022).
- [10] M. Millot, S. Zhang, D.E. Fratanduono, F. Coppari, S. Hamel, B. Militzer, D. Simonova, S. Shcheka, N. Dubrovinskaia, L. Dubrovinsky, J.H. Eggert. Geophys. Res. Lett. **47**, 4, e2019GL085476 (2020).
- [11] R.M. Bolis. Investigations of high pressure phase diagrams of MgO– SiO_2 systems with laser shock compression. Physics. Université Paris Saclay (COMUE), English. NNT: 2017SACLX056 (2017).
- [12] D.K. Spaulding, R.S. McWilliams, R. Jeanloz, J.H. Eggert, P.M. Celliers, D.G. Hicks, G.W. Collins, R.F. Smith. Phys. Rev. Lett. **108**, 6, 065701 (2012).
- [13] P.I. Dorogokupets, A.M. Dymshyts, T.S. Sokolova, B.S. Danilov, K.D. Litasov. Geologiya i geofizika, **56**, 1–2, 224 (2015). (in Russian).
- [14] R.M. Bolis, G. Morard, T. Vinci, A. Ravasio, E. Bambrink, M. Guarguaglini, M. Koenig, R. Musella, F. Remus, J. Bouchet, N. Ozaki, K. Miyaniishi, T. Sekine, Y. Sakawa, T. Sano, R. Kodama, F. Guyot, A. Benuzzi-Mounaix. Geophys. Res. Lett. **43**, 18, 9475 (2016).

- [15] R. Musella, S. Mazevet, F. Guyot. Phys. Rev. B **99**, 6, 064110 (2019).
- [16] L.V. Altshuler, R.F. Trunin, G.V. Simakov. Izv. AN SSSR. Ser. Fizika Zemli, **29**, 10, 1 (1965). (in Russian).
- [17] R.F. Trunin. Issledovaniya ekstremal'nykh sostoyanii kondensirovannykh veshchestv metodom udarnykh voln. Uravneniya Gyugonio. RFYATs-VNIIEF, Sarov (2006) 286 p. (in Russian).
- [18] M.A. Podurets, G.V. Simakov, R.F. Trunin. Izv. AN SSSR **4**, 28 (1968). (in Russian).
- [19] K.K. Maevskii. Tech. Phys. **66**, 6, 749 (2021).
- [20] K.K. Maevskii. Tech. Phys. **67**, 12, 1580 (2022).
- [21] K.K. Maevsky. Vestn. Tomskogo gos. un-ta. Matematika i mekhanika **79**, 111 (2022). (in Russian).
- [22] V.V. Milyavskii, V.E. Fortov, A.A. Frolova, K.V. Khishchenko, A.A. Charakhch'yan, L.V. Shurshalov. Computat. Math. Mathemat. Phys. **46**, 5, 873 (2006).
- [23] K.K. Maevskii. J. Phys. Conf. Ser. **894**, 1, 012057 (2017).
- [24] K.K. Maevskii. AIP Conf. Proc. **2051**, 1, 020181 (2018).
- [25] K.K. Maevskii, S.A. Kinelovskii. AIP Conf. Proc. **1783**, 1, 020143 (2016).
- [26] K.K. Maevskii, S.A. Kinelovskii. High Temperature **56**, 6, 853 (2018).
- [27] K. Maevskii. AIP Conf. Proc. **2103**, 1, 020009 (2019).
- [28] Compendium of shock wave data / Ed. M. Thiel. Report UCRL-50108, Livermore, Lawrence Livermore Laboratory (1977). 401 p.
- [29] K. Miyanishi, Y. Tange, N. Ozaki, T. Kimura, T. Sano, Y. Sakawa, T. Tsuchiya, R. Kodama. Phys. Rev. E **92**, 2, 023103 (2015).
- [30] A.M. Dziewonski, D.L. Anderson. Phys. Earth Planet. Int. **25**, 4, 297 (1981).
- [31] LASL Shock Hugoniot Data / Ed. S.P. Marsh. Univ. California Press, Berkeley (1980). 658 p.
- [32] R.F. Trunin, L.F. Gudarenko, M.V. Zhernokletov, G.V. Simakov. Eksperimental'nye dannye po udarno-volnovomu szhatiyu i adiabaticheskomu rasshireniyu kondensirovannykh veshchestv. RFYATs-VNIIEF, Sarov (2006) 531 p. (in Russian).
- [33] M.A. Podurets, G.V. Simakov, R.F. Trunin. Izv. AN SSSR. Ser. Fizika Zemli, **4**, 28 (1968). (in Russian).
- [34] Yu.N. Zhugin, K.K. Krupnikov, N.A. Ovechkin, E.V. Abashkin, M.M. Gorshkov, V.T. Zaikin, V.T. Slobodenyukov. Izv. AN SSSR. Ser. Fizika Zemli, **16**, 1994 (1). (in Russian).
- [35] G.A. Adadurov, A.N. Dremin, S.V. Pershin, V.N. Rodionov, Yu.N. Ryabinin. PMTF4, 81 (1962). (in Russian).
- [36] J.L. Mosenfelder, P.D. Asimow, D.J. Frost, D.C. Rubie, T.J. Ahrens. J. Geophys. Res. **114**, B1, B01203 (2009).
- [37] Y. Fei. Nature Commun. **12**, 876 (2021).
- [38] D.K. Spaulding, R.S. McWilliams, R. Jeanloz, J.H. Eggert, P.M. Celliers, D.G. Hicks, G.W. Collins, R.F. Smith. Phys. Rev. Lett. **108**, 6, 065701 (2012).

Translated by E.Ilyinskaya